

Supporting Information

Extended π -conjugated cores on arylamine derivatives-based hole-transporting materials for perovskite solar cells: theoretical design and experimental research

Qian Chen, Hongyuan Liu, Puhang Cheng, Xiaorui Liu*

Key Laboratory of Luminescence Analysis and Molecular Sensing, Ministry of Education, School of Chemistry and Chemical Engineering, Southwest University, Chongqing 400715, P.R. China

*Corresponding authors: Xiaorui Liu; E-mail addresses: liuxiaorui@swu.edu.cn (X. Liu)

Contents:

- 1. Computational details**
- 2. Experimental section**
- 3. Target molecule synthesis**
- 4. Experimental characterization**
- 5. References**

1. Computational details

1.1 Geometry optimization and electronic properties

In order to choose a suitable method (which is accordance with the experiment value), we tested a series of functional, including B3LYP, B3P86, BMK and PBE0, to optimize the ground-state (S_0) geometry of investigated model compound Spiro-OMeTAD using the 6-311G(d,p) basis set (Table S1). The results indicate that the HOMO energy level of Spiro-OMeTAD (-5.06 eV) computed at B3P86/6-311G(d,p) level agree with the experiment value (-5.13 eV)¹ very well. So, we optimize the S_0 geometry of investigated molecules CQ4-CQ6 using the B3P86/6-311G(d,p) method and basis set.² The energies of all of the obtained geometries are ensured to be the lowest because the optimized structures do not exhibit imaginary frequency. The vibrational analysis was also using the same theoretical level to guarantee that the optimized geometry (Fig. S1) was the minimum of potential energy surface. Moreover, energy calculations, including electron affinities, adiabatic ionization potential and absolute hardness of the investigated systems, were performed using the PBE0/6-31G(d) method. The solvation free energy for all molecules was calculated using the TD-PBE0/6-31G(d) method in chlorobenzene solution or in gas.

1.2 Calculations of optical absorption

The absorption spectrum at the optimized ground-state geometry of Spiro-OMeTAD with the 30 lowest singlet-singlet excitations was calculated using the time-dependent density functional theory (TD-DFT) method. The optical absorptions of Spiro-OMeTAD were simulated by TD-DFT with B3P86, B3LYP, PBE0 and BMK at 6-31G(d) level in dichloromethane solution with a polarizable continuum model (PCM).³ The maximum absorption of Spiro-OMeTAD for B3P86, B3LYP, PBE0 and BMK methods are 403, 402, 388 and 355 nm, respectively. The calculated result

shows that maximum absorption wavelength ($\lambda_{\text{abs,cal}}$) of Spiro-OMeTAD (388 nm) from the TD-PBE0/6-31G(d) calculations is in line with that of experimental value (386 nm).¹ Therefore, the optical properties of CQ4-CQ6 are calculated by TD-PBE0/6-31G(d) functional and basis set in dichloromethane solution.

1.3 Calculations of charge mobility

In this work, we make use of the first-principles simulation to quantitative prediction of charge mobility, this method was also used in the previous work and confirmed.⁴ This simulation model is based on a combination of first-principles quantum mechanics calculations and Marcus theory. By using the hopping mechanism to describe the charge transfer, the parameter of charge transfer rate (k) for organic molecules can be calculated from the Marcus–Hush equation:⁵

$$k = \frac{v^2}{h} \sqrt{\frac{4\pi^3}{\lambda k_B T}} \exp\left(\frac{-\lambda}{4k_B T}\right) \quad (\text{S1})$$

Where h is the Planck's constant, v is the electronic coupling between adjacent molecules in the crystal structure (use ADF to calculate), λ is the reorganization energy,⁶ k_B is the Boltzmann constant, T is the temperature (in this calculation is set to 298 K). It's reported that descriptions of the charge transfer on basis of the hopping mechanism was universally accepted. In equation (S1), the parameters such as λ and v are the key factors to determine the transfer rate of organic materials. In equation (S1), for an optimal transport system, electronic coupling should be maximized and λ should be minimized.

The inner reorganization energy (λ) is obtained from the adiabatic potential energy surface method, be calculated as follows:

$$\lambda = (E_0^* - E_0) + (E_+^* - E_+) \quad (\text{S2})$$

Where E_+^* represent the total energy of the neutral segment from the geometries of cation segment. E_0^* represent the total energy of the cation segment from the geometries of neutral segment. E_+ is the total energy of the cation segment in the lowest energy geometries. E_0 is the total energy of the neutral segment in the lowest energy geometries.⁷ Energies of the neutral segment and the cation segment for inner reorganization energy of HTMs were performed using the B3P86/6-311G(d,p) method and basis set.

The parameter of electronic coupling (v) could be obtained from the equation as shown below:⁸

$$v = \frac{J_{RP} - S_{RP}(H_{RR} + H_{PP})/2}{1 - S_{RP}^2} \quad (S3)$$

where S_{RP} and J_{RP} are the spatial overlap and charge transfer integral, respectively. H is the site energies (H_{RR} and H_{PP}). The parameter of J_{RP} could be simulated by the equation as shown below:⁸

$$J_{RP} = \langle \varphi_{HOMO}^1 | h_{ks} | \varphi_{HOMO}^2 \rangle \quad (S4)$$

where h_{ks} is the Kohn-Sham Hamiltonian between two fragments. The parameters such as φ_{HOMO}^1 and φ_{HOMO}^2 are the HOMOs of two fragments, respectively.

The hole mobility of the designed HTMs was calculated from the Einstein relation:⁹

$$\mu = \frac{1}{2n} \frac{e}{k_B T} \sum_i r_i^2 k_i P_i \quad (S5)$$

where n is the spatial dimensionality, e is the electron charge, i is a selected hopping pathway and r_i is the charge hopping centroid to centroid distance, k_i and P_i are the charge transfer rate (k) and hopping probability, respectively. P_i can be expressed as:

$$P_i = \frac{k_i}{\sum_i k_i} \quad (S6)$$

Han et al.⁴ presented a model to simulate the anisotropic mobility (μ_Φ) by projecting the different hopping pathways.

The equation of angular resolution anisotropic mobility can be described as follows:

$$\mu_\Phi = \frac{e}{2k_B T} \sum_i K_i r_i^2 P_i \cos^2 \gamma_i \cos^2 (\theta_i - \Phi) \quad (S7)$$

Where r_i , γ_i , and θ_i reveal the intermolecular packing parameters in the organic crystals. γ_i is the angle of the hopping pathway relative to the transport plane of the organic crystal molecular stacking layer, θ_i and Φ are defined as the orientation angle of the projected electronic coupling pathways of different dimer types and the conducting channel relative to the same reference axis (commonly using the crystallographic axis), respectively. Thus, the angle between the different pathways and the conducting channel is $(\theta_i - \Phi)$.

The electronic coupling could be simulated from the PW91/TZP levels in ADF program.¹⁰⁻¹³

The DFT and TD-DFT calculations were carried out by the Gaussian 09 program.¹⁴

1.4 Simulation of crystal structures

In order to calculate the parameter of electronic coupling for HTMs, it was compelled to obtain the dimer structure, which was defined as adjacent segments from the crystal structures of molecules. The crystal structure of the investigated HTMs can be predicted from the polymorph module in Material Studio software.⁸ The geometry of the cluster models used in the present study was taken from the B3P86/6-311G(d,p) level. The Deriding force field was used for the prediction.¹⁵ For the investigated molecules, the polymorph calculations are restricted to the six most probable space groups such as $P2_1/c$, $P1$, $P2_12_12_1$, $C2/c$, $P2_1$ and $Pbca$.¹⁶ Then, the crystal structures were sorted according to their total energy. On basis of the crystal structures, we selected a molecule as center. All of the adjacent fragments with the center are defined as the transport pathways. To obtain

their spatial parameters, a molecule was selected discretionarily as the center of hole transporting, and the adjacent molecules were represented as dimers in different directions which marked as P, T, L. The angle between each jump path and the coordinate axis were labeled θ_p , θ_{Ti} , θ_{Li} . The angle of the final transmission direction relative to the reference axis was defined as Φ . γ was the angle of the hopping pathway relative to the transport plane of the organic crystal molecular stacking layer. To determine the hole transport plane, various planes of each molecule were considered, and the electronic coupling of each dimers in each plane was theoretically calculated. Then, the hole mobility of each plane was calculated using the above formula, and the plane with the largest hole mobility was defined as the final transport plane (Fig. 3).

2. Experimental section

2.1 Materials

All starting reagents and solvents were used as received from commercial sources and used as received unless specially stated. Including 3,6,11,14-tetrabromodibenzo[g,p]chrysene, 4-methoxy-N-(4-methoxyphenyl)-N-(4-(4,4,5,5-tetramethyl-1,3,2-dioxaborolan-2-yl) phenyl) aniline. FAI, MABr, Indium tin oxide (ITO) coated glass, PbI_2 (99.999%) and $PbBr_2$ (99.999%) were purchased from Advanced Election Technology CQ., Ltd. Spiro-OMeTAD (99.5%) and PEDOT:PSS (Heraeus, Clevis PVP Al 4083) were purchased from *p*-OLED (China). Lithiumbis-(trifluoromethylsulfonyl)imide (LiTFSI,99%), 4-(tert-Butyl)pyridine (TBP, 99%), CsI (99%), were purchased from *p*-OLED (China). Anhydrous DMSO (99.8%), DMF (99.8%) and chlorobenzene (99.8%) were purchased from Sigma Aldrich. Solvents for chemical synthesis such as DMF and DCM were treated according to the standard procedures.

2.2 Device fabrication

We fabricated n-i-p PSCs with a structure of FTO-TiO₂/CsFAMA/HTMs/Ag to measure the photovoltaic performance of PSCs. Patterned FTO-TiO₂ glass were used as received from commercial sources (Advanced Election Technology CQ., Ltd). A perovskite precursor solution (1.30 M PbI₂, 1.19 M FAI, 0.14 M PbBr₂, 0.14 M MABr, and 0.07 M CsI in DMF:DMSO mixed solution with a v/v of 4:1) was spin-coated in a two-step program at 1000 and 6000 rpm for 10 and 30 s, respectively. During the second step, 100 μ L of chlorobenzene was dropped on the spinning substrate at 15 s after the start-up. Next, the as-spun perovskite layer was annealed on a hot plate at 120 °C for 60 min to drive off solvent and form the perovskite phase.

The hole-transporting layers (HTLs) were deposited by spin-coating with 30 s (6000 rpm for Spiro-OMeTAD, 3000 rpm for CQ4) corresponding solution on top of perovskite films. The HTM solution was each prepared by dissolving Spiro-OMeTAD (72.3 mg) in 1 mL chlorobenzene, 28.8 mL tert-butylpyridine (TBP) solution and 17.5 mL lithium bis(trifluoro methylsulfonyl) imide (Li-TFSI)/acetonitrile (520 mg/1 mL). CQ4 dissolved in chlorobenzene in a concentration of 30 mg mL⁻¹, with tBP and Li-TFSI as dopants. After oxidizing the HTM layers in air for 15 h, the devices were pumped to lower than 10⁻⁵ torr and an approximately 100 nm thick Ag counter electrode was deposited on top. The active area of our device is 0.06 cm².

2.3 The space-charge-limited current (SCLC) hole mobility measurements

Hole-only devices are fabricated with the structure ITO/PEDOT:PSS/HTM/MoO₃/Ag. The dark $J-V$ characteristics of hole-only devices were measured under N₂ atmosphere inside a glove box. PEDOT:PSS was deposited on the ITO substrate at 5000 rpm for 30 s, followed by annealing at 120 °C for 30 min and the conditions of spin coating HTM are consistent with the device fabrication. Mobility is extracted by fitting the current density-voltage curves using space charge

limited current (SCLC). Fitting the results to a space charge limited form, based on the following equation $J = 9\varepsilon_{\theta}\varepsilon_{\gamma}\mu_h V^2 / 8L^3$. J is the current density, L is the film thickness of the active layer, μ_h is the hole mobility, ε_{γ} is the relative dielectric constant of the transport medium, ε_{θ} is the permittivity of free space (8.85×10^{-12} F m⁻¹), V is the internal voltage of the device.

2.4 Measurements

The nuclear magnetic resonance (NMR) spectra were obtained from a BRUKER AVANCE III 600 MHz NMR Instrument (in CDCl₃ or in DMSO). Mass spectra were collected on a Bruker impact II high-resolution mass spectrometer. MALDI-TOF HRMS was performed on a Bruker Autoflex instrument, using 1,8,9-trihydroxyanthracene as a matrix. UV-vis absorption spectra were measured on a Shimadzu UV-2450 absorption spectrophotometer. Cyclic voltammetry studies were conducted using a CHI660E system in a typical three-electrode cell with a glass carbon working electrode, a platinum wire counter electrode, and a silver/silver chloride (Ag/AgCl) reference electrode. All electrochemical experiments were carried out under a nitrogen atmosphere at room temperature in an electrolyte solution of 0.1 M tetrabutylammonium hexa-fluorophosphate (Bu₄NPF₆) in dichloromethane at a sweeping rate of 50 mV s⁻¹. The potential of Ag/AgCl reference electrode was internally calibrated by using the ferrocene/ferrocenium redox couple (Fc/Fc⁺). According to the onset oxidation potential of the CV measurements, the highest occupied molecular orbital (HOMO) was estimated based on the vacuum energy level of ferrocene (5.1 eV): HOMO = $-(E_{\text{onset}} - E_{\text{Fc/Fc}^+}) - 5.1$ eV. Using atomic force microscopy (AFM) to characterize the morphology, the model is CSPM5500A. Steady-state PL spectra were recorded on Fluorolog®-3 fluorescence spectrometer (Horiba). Time-resolved PL decay curves were measured by a single photon counting spectrometer from Horiba Instruments (Fluorolog®-3) with a Picosecond Pulsed UV-LASTER

(LASTER375) as the excitation source. The current–voltage (J – V) curves were measured under 100 mW cm⁻² (AM 1.5 G) simulated sunlight using Keithley 2400 in conjunction with a Newport solar simulator (94043A). Film thickness of hole transport layer and perovskite layer were measured by Surfcoorder ET150, Kosaka Laboratory Ltd.

3. Target molecule synthesis

Synthesis of 4,4',4'',4'''-(dibenzo[g,p]chrysene-3,6,11,14-tetrayl)tetrakis(N,N-bis(4-methoxyphenyl)aniline) (CQ4): The compound 1 (0.2443 g, 0.189 mmol) and the compound 2 (0.4107 g, 0.95 mmol) were accurately weighed and put into the reaction flask, the catalyst Pd(PPh₃)₄ (0.057 g, 0.05 mmol) was added under a nitrogen atmosphere, the system was vacuum replaced three times, and the DMF (15 mL) and potassium carbonate solution (2M 5 ml) prepared by deoxygenation in advance were added. The reaction was refluxed at 95 °C for 24 h. Cool to room temperature, quench the reaction with water, dry with anhydrous sodium sulfate and extract the organic solvent with dichloromethane. The crude product was purified by column chromatography on silica gel. CQ4: yield: 88% (258 mg) as a yellow solid. ¹H NMR (600 MHz, DMSO-d₆) δ 9.05 (s, 1H), 8.62 (d, J = 8.8 Hz, 1H), 7.94 (d, J = 8.4 Hz, 1H), 7.84 (d, J = 8.2 Hz, 2H), 7.09 (d, J = 8.3 Hz, 4H), 6.96 (d, J = 8.3 Hz, 4H), 6.92 (d, J = 8.1 Hz, 2H), 3.60 (s, 2H). ¹³C NMR (151 MHz, Chloroform-d) δ 138.45, 128.16, 127.45, 125.45, 121.40, 114.58, 114.30, 55.50. HR-MS: m/z = 1541.6344, calcd for C₁₀₆H₈₄N₄O₈: 1541.6323.

4. Experimental characterization

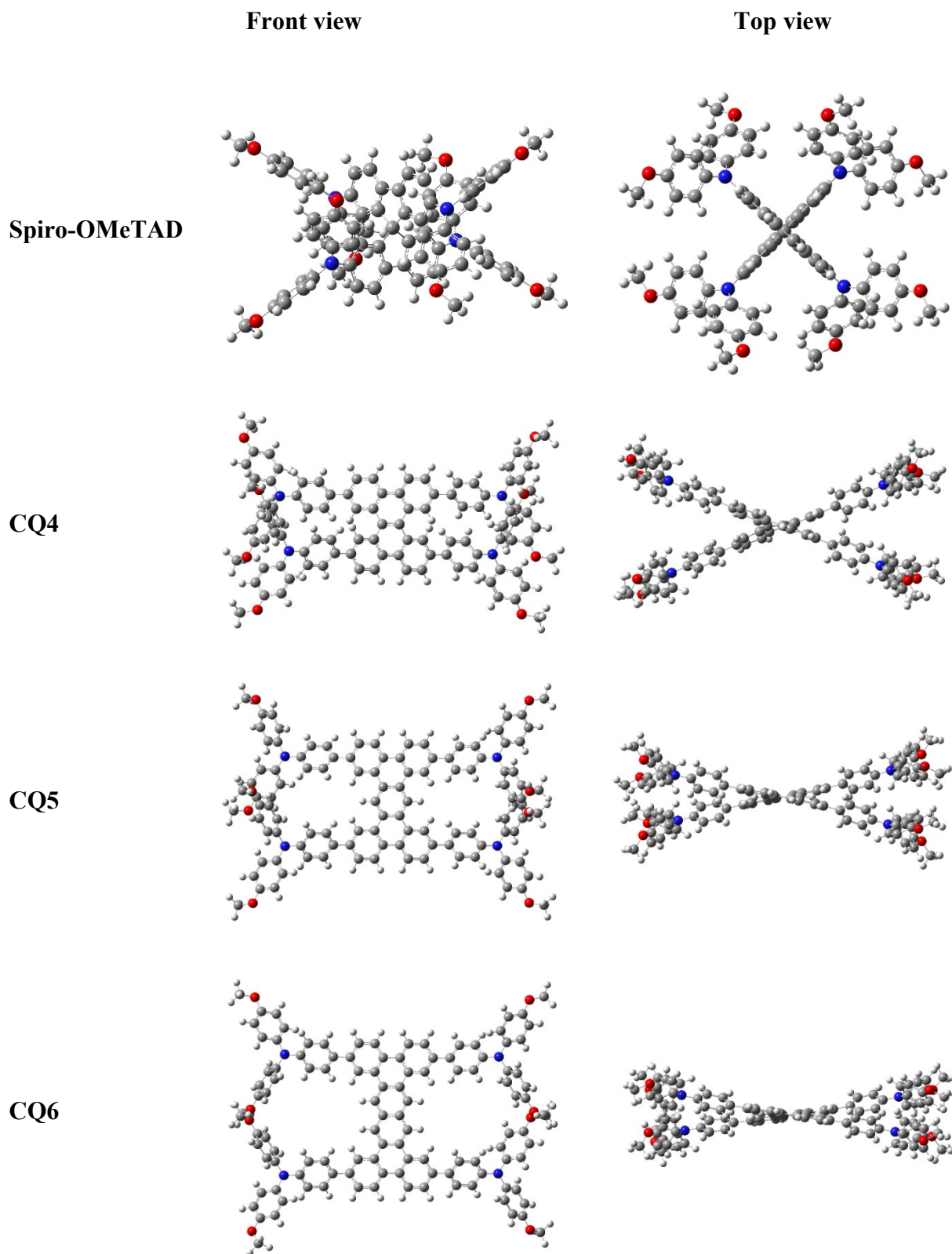


Fig. S1 Optimized geometries of the investigated molecules in this work as obtained using the B3P86/6-311G(d,p) method.

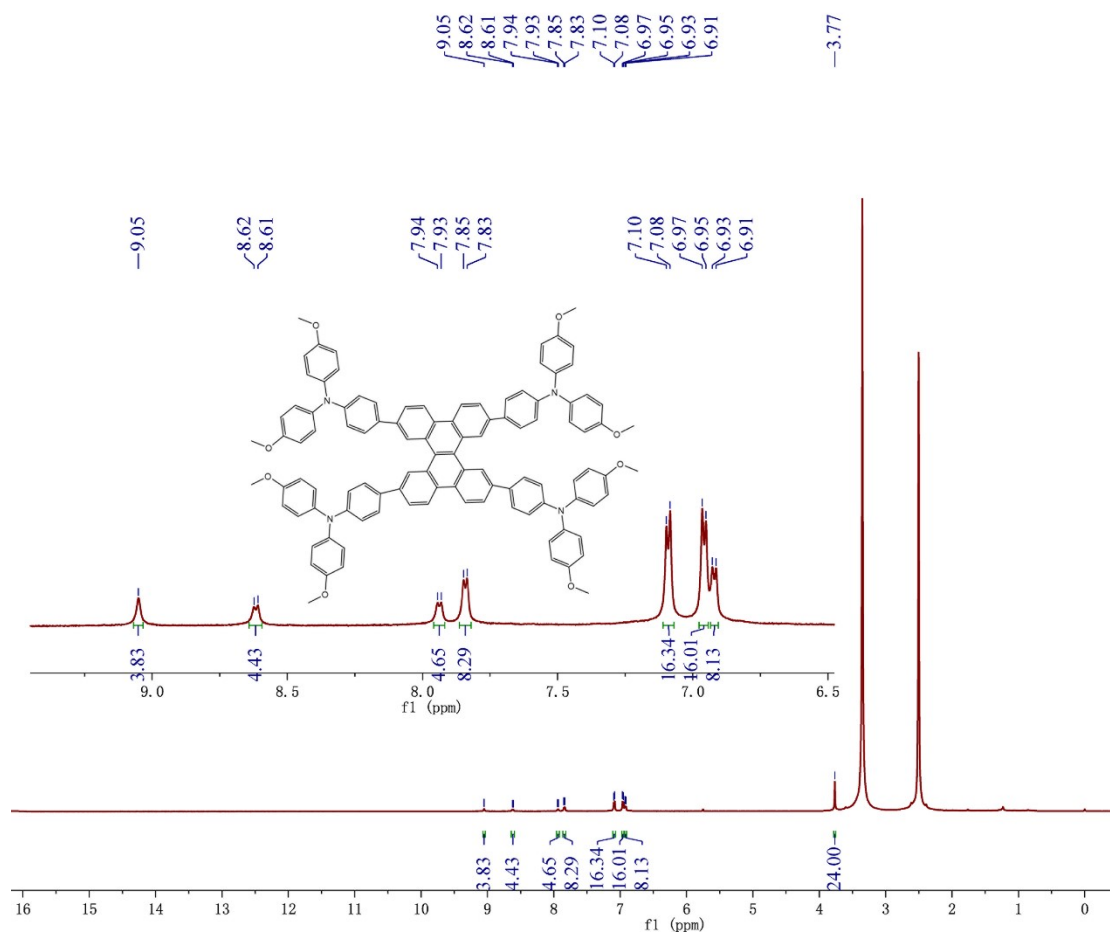


Fig. S3 ¹H NMR spectrum of CQ4 in DMSO.

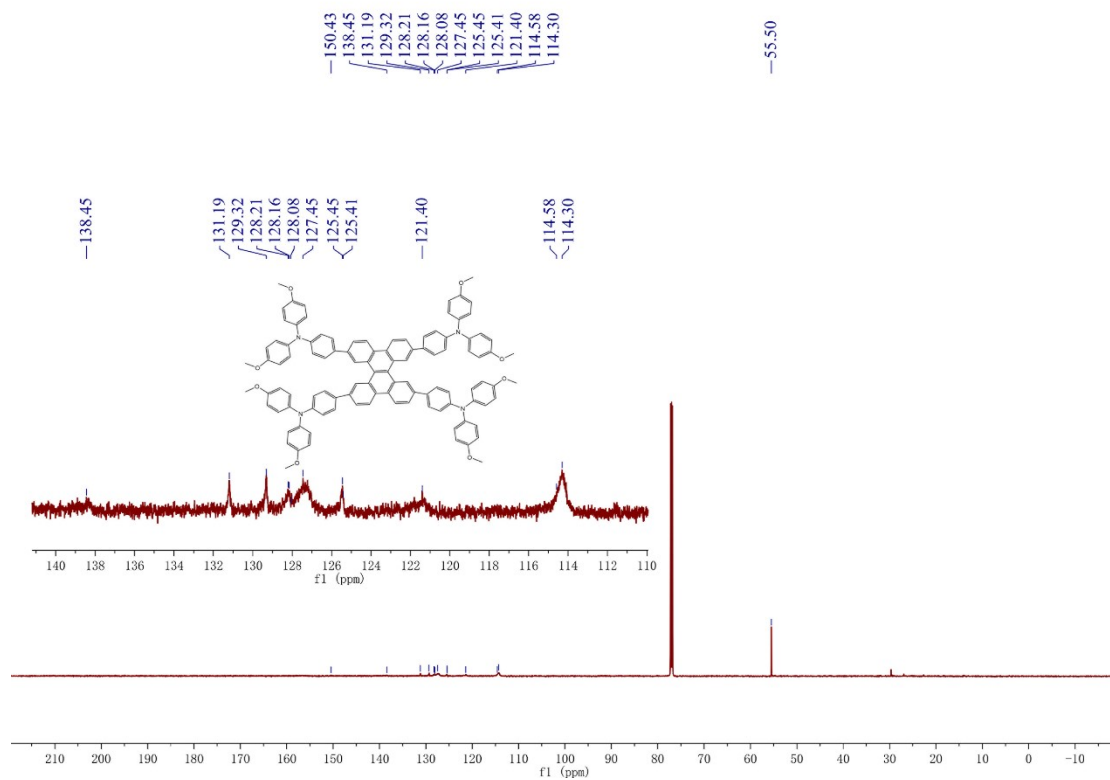


Fig. S4 ¹³C NMR spectrum of CQ4 in CDCl₃.

System Verification of Internal Mass Accuracy ESI Mode

Analysis Info

Analysis Name D:\Data\QL\1000_0_A21_000008.d
 Method 4-13-DaDou
 Sample Name
 Comment Glu-Fib 250amol

Acquisition Date 5/21/2021 10:58:18 PM

Operator
 Instrument solariX

Acquisition Parameter

Polarity	Positive	n/a	n/a	No. of Laser Shots	100
n/a	n/a	No. of Cell Fills	1	Laser Power	70.0 Ip
Broadband Low Mass	53.8 m/z	n/a	n/a	n/a	n/a
Broadband High Mass	3000.0 m/z	n/a	n/a	n/a	n/a
Acquisition Mode	Single MS	n/a	n/a	Calibration Date	Fri Feb 21 02:36:54 2014
Pulse Program	basic	n/a	n/a	Data Acquisition Size	1048576
Source Accumulation	0.100 sec	n/a	n/a	Apodization	Sine-Bell Multiplication
Ion Accumulation Time	0.500 sec	n/a	n/a		
Flight Time to Acq. Cell	0.001 sec				

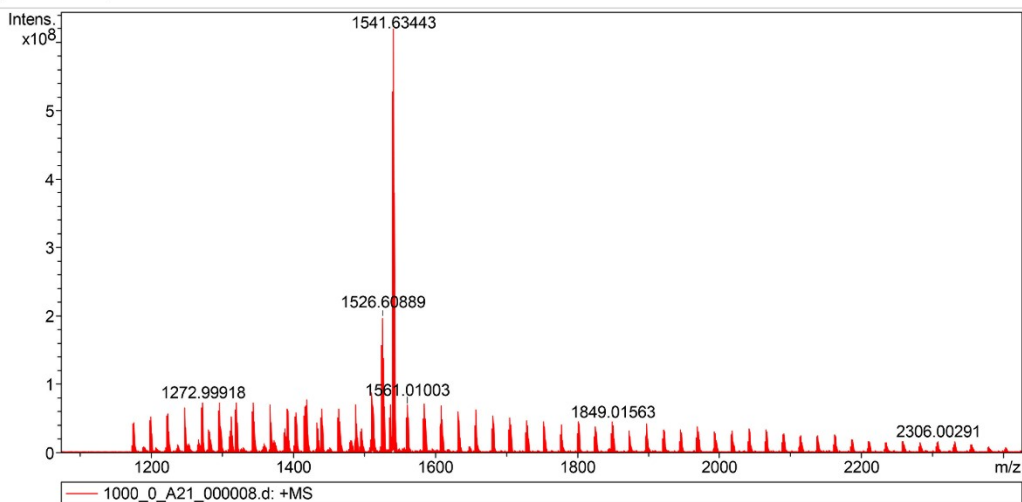


Fig. S5 High resolution mass spectrometry of CQ4.

MASS SPECTROMETRY REPORT

Sample No.	Formula (M)	Measured m/z	Calc. m/z	Diff (ppm)
CQ4	C ₁₀₆ H ₈₄ N ₄ O ₈	1541.6344	1541.6323	1.36

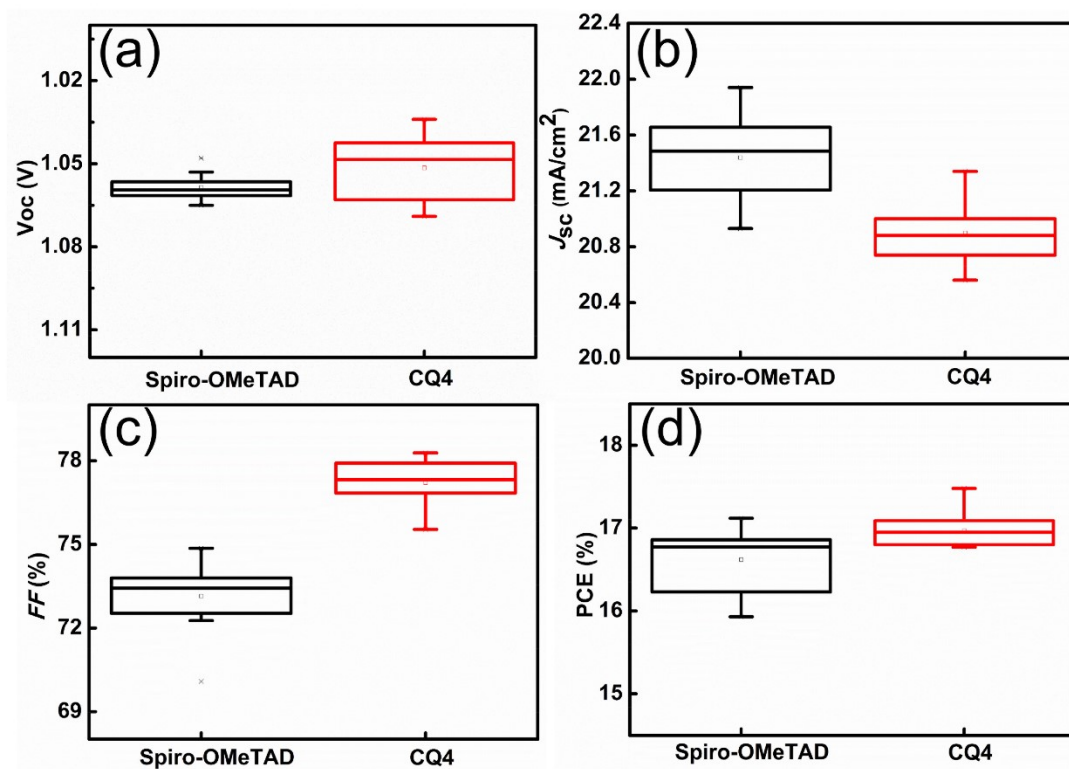


Fig. S6. Box charts of the photovoltaic parameters of Spiro-OMeTAD and CQ4.

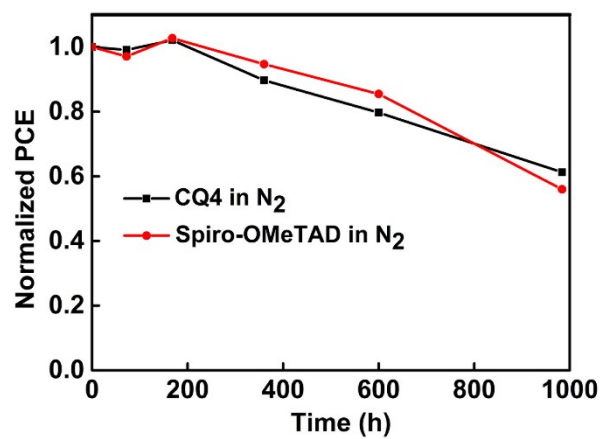


Fig. S7. Stability test of PSCs based on Spiro-OMeTAD or CQ4 under in N_2 glove box at dark room with ~ 298 K of temperature and 10%~35% of humidity.

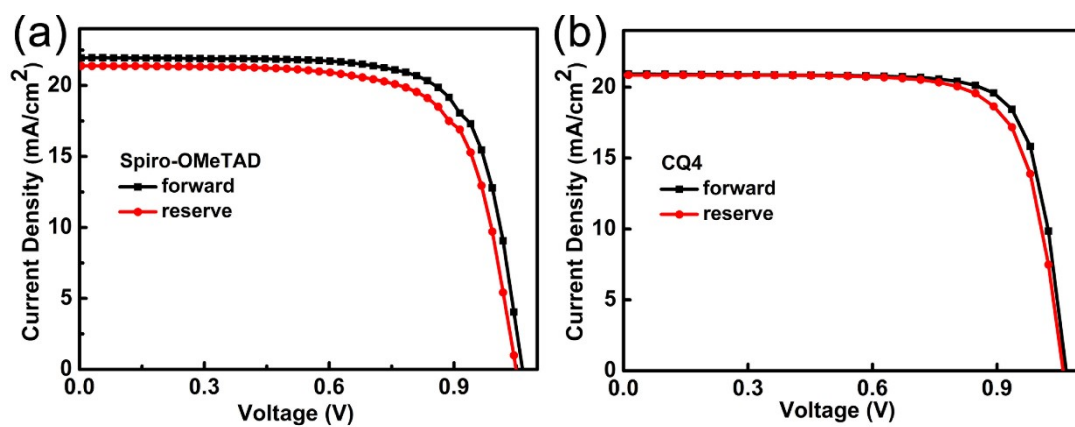


Fig. S8. J - V curves measured under reverse and forward voltage scans with Spiro-OMeTAD (a) or CQ4 (b) as HTMs.

Table S1. The HOMO and the LUMO values obtained with B3P86, B3LYP, BMK and PBE0 methods (6-311G** basis set was used) of Spiro-OMeTAD.

Spiro-OMeTAD	Spiro-OMeTAD (exp ^a)	B3P86	B3LY P	BMK	PBE0
HOMO/eV	-5.13	-5.06	-4.67	-5.06	-4.77
LUMO/eV	-2.08	-2.09	-1.65	-1.16	-1.66

^a from ref.¹

Table S2. The HOMO, LUMO and energy gap of Spiro-OMeTAD and CQ4-CQ6 from theoretical calculations.

	Spiro-OMeTAD (exp.) ^a	Spiro-OMeTAD b	CQ4 ^b	CQ5 ^b	CQ6 ^b
HOMO/eV	-5.13	-5.06	-5.22	-5.25	-5.26
LUMO/eV	-2.08	-2.09	-2.49	-2.50	-2.82
E _g /eV	3.05	2.97	2.73	2.75	2.44

^a from ref.¹

^bThe HOMO and LUMO energy calculated by B3P86/6-311G(d,p) is fitted according to the formula:²

$$\text{HOMO}(\text{exp}) = 0.66 \text{ HOMO}(\text{th.}) - 1.75 \quad (\text{R}=0.79)$$

$$\text{LUMO}(\text{exp}) = 0.69 \text{ LUMO}(\text{th.}) - 1.07 \quad (\text{R}=0.88)$$

Table S3. Predicted crystal data of Spiro-OMeTAD and CQ4-CQ6.

Compounds	Space group	a(Å)	b(Å)	c(Å)	α(°)	β(°)	γ(°)
Spiro-OMeTAD	<i>PI</i>	14.641673	16.990535	14.726886	101.4063	90.00782	93.6173
CQ4	<i>PI</i>	14.476829	48.306241	11.672031	68.47035	57.09144	45.84997
CQ5	<i>PI</i>	17.315051	12.355247	30.408119	63.50929	95.93435	70.8086

Table S4. Summary of hysteresis index (HI) and device performance of perovskite solar cell adopting different hole transporting materials at forward and reverse voltage scans.

HTM		V_{oc} [V]	J_{sc} [mA cm ²]	FF [%]	PCE [%]	HI ^a [%]
Spiro-OMeTAD	forward	1.064	21.94	73.30	17.12	6.66
	reverse	1.049	21.38	71.26	15.98	
CQ4	forward	1.066	20.94	78.28	17.48	4.81
	reverse	1.059	20.85	75.32	16.64	

$$^a\text{HI} = [(PCE_{\text{forward}} - PCE_{\text{reverse}})/PCE_{\text{forward}}] \times 100\%$$

5. References

1. B. Xu, Z. Zhu, J. Zhang, H. Liu, C.-C. Chueh, X. Li and A. K. Y. Jen, *Adv. Energy Mater.*, 2017, **7**, 1700683.
2. X. R. Liu and X. Liu, *RSC Adv.*, 2019, **9**, 24733-24741.
3. J. Tomasi, B. Mennucci and R. Cammi, *Chem. Rev.*, 2005, **105**, 2999-3094.
4. W. Q. Deng, L. Sun, J. D. Huang, S. Chai, S. H. Wen and K. L. Han, *Nat. Protoc.*, 2015, **10**, 632-642.
5. R. A. Marcus, *Annu. Rev. Phys. Chem.*, 1964, **15**, 155-196.
6. V. Coropceanu, J. Cornil, D. A. da Silva Filho, Y. Olivier, R. Silbey and J.-L. Brédas, *Chem. Rev.*, 2007, **107**, 926-952.
7. B. C. Lin, C. P. Cheng and Z. P. M. Lao, *J. Phys. Chem. A*, 2003, **107**, 5241-5251.
8. K. Senthilkumar, F. Grozema, F. Bickelhaupt and L. Siebbeles, *J. Chem. Phys.*, 2003, **119**, 9809-9817.
9. W. Q. Deng and W. A. Goddard, *J. Phys. Chem. B*, 2004, **108**, 8614-8621.
10. ADF2014 SCM Theoretical Chemistry, Vrije Universiteit, Amsterdam, The Netherlands (<http://www.scm.com>).
11. G. te Velde, F. M. Bickelhaupt, E. J. Baerends, C. Fonseca Guerra, S. J. A. van Gisbergen, J. G. Snijders and T. Ziegler, *J. Comput. Chem.*, 2001, **22**, 931-967.
12. J. P. Perdew, J. A. Chevary, S. H. Vosko, K. A. Jackson, M. R. Pederson, D. J. Singh and C. Fiolhais, *Phys Rev B Condens Matter*, 1992, **46**, 6671-6687.
13. C. Fonseca Guerra, J. G. Snijders, G. te Velde and E. J. Baerends, *Theor. Chem. Acc.*, 1998, **99**, 391-403.
14. M. J. Frisch, G. W. Trucks, H. B. Schlegel, G. E. Scuseria, M. A. Robb, J. R. Cheeseman, G. Scalmani, V. Barone and G. A. Petersson, Fox, "Gaussian 09," Revision A.1, Gaussian, Inc., Wallingford, 2009.
15. R. F. Jin and Y. F. Chang, *Phys. Chem. Chem. Phys.*, 2015, **17**, 2094-2103.
16. W.-J. Chi and Z.-S. Li, *Phys. Chem. Chem. Phys.*, 2015, **17**, 5991-5998.